Journal of Physics and Chemistry of Solids 71 (2010) 1381–1387

Contents lists available at ScienceDirect

Journal of Physics and Chemistry of Solids

journal homepage: www.elsevier.com/locate/jpcs

Structural and optical properties of $In_{35}Sb_{45}Se_{20-x}Te_x$ phase-change thin films

A.K. Diab *, M.M. Wakkad, E.Kh. Shokr, W.S. Mohamed

Physics Department, Faculty of Science, Sohag University, 82524 Sohag, Egypt

ARTICLE INFO

Article history:
Received 12 December 2009
Received in revised form
8 June 2010
Accepted 25 June 2010

Keywords:
A. Chalcogenide
A. Glasses
A. Thin films
B. X-ray diffraction
D. Optical properties

ABSTRACT

Physical properties of $In_{35}Sb_{45}Se_{20-x}Te_x$ thin films with different compositions (x=2.5, 5, 7.5, 10, 12.5 and 15 at%) prepared by electron beam evaporation method are studied. X-ray diffraction results indicate that the as-evaporated films depend on the Te content and the crystallized compounds consist mainly of Sb_2Se_3 with small amount of Sb_2SeTe_2. Transmittance and reflectance of the films are found to be thickness dependent. Optical-absorption data indicate that the absorption mechanism is direct transition. Optical band gap values decrease with increase in Te content as well as with increase in film thickness.

Published by Elsevier Ltd.

1. Introduction

The phase change material is a kind of new material rapidly developing in recent years with wide application fields. Phase change materials, based on their reversible switch between the amorphous and crystalline states, have been used for optical rewritable data storage media [1–3]. Recently, they were also shown to exhibit a great potential for use in future electronic nonvolatile memory devices, the so-called phase change random access memory (PRAM) [4–6]. A focused laser beam is employed as a heat source for optical data storage applications, while a current pulse is used to heat the active layer of PRAM devices. The amorphous and crystalline states of the phase change recording layer are distinguished by their pronounced difference in reflectivity or electrical conductivity to read the recorded data. In the last decade, many researchers have concentrated on optical properties and alloys with a focus on disc performance. It was postulated that the reversible transformation of amorphous-to-polycrystalline phases might be correlated with optical applications [7–9]. In–Sb alloy is one of the most important III–V semiconductor compounds, which possesses two outstanding characters: very small forbidden band width (0.18 eV at room temperature) [10] and very small effective mass of electron (about 1.5% of free electron mass) [11]. The absorption spectrum of amorphous In–Sb thin films is also noticeable for its very steep threshold value close to the higher energy side. Doped with Te the absorption limitation moves from 0.18 to 0.6 eV [12]. To the authors' knowledge, ternary compounds In–Sb–Te as direct overwritable phase-change optical data storage materials in the near infrared wavelength region have been reported previously [13,14], while reports on the optical recording performance of In–Sb–Te alloy films at short-wavelength region (especially 514.5 nm) have not been found. Some authors studied physical properties of the In–Sb–Se system [15–17]. Few authors studied the optical properties [18]. Studies on Sb–Te–Se compounds are very useful because the compounds could be made into erasable optical recording media. Phase-change material systems such as In–Sb–Se, In–Sb–Te, Ge–Te–Sb and Ag–In–Sb–Te [19] were studied. Glass-formation, amorphization range and the information recording conditions for the amorphous layers of In–Sb–Se system (Sb–Se and Sb_2Se_3–InSb section and the conditions of optical information recording on amorphous layers of $(Sb_2Se_3)_x(InSb)_{1-x}$ were studied [20]. In $(Sb_2Se_3)_x(InSb)_{1-x}$ system the difference in reflectance of the crystallized and amorphous areas increases with InSb content and is maximal for the $In_{35}Sb_{45}Se_{20}$ composition. It should be noted that the reflectance difference in $(Sb_2Se_3)_x(InSb)_{1-x}$ films is several times higher than in Sb_xSe_{1-x} films [20]. The aim of this work is to study the effect of Te doping on structure and optical properties of the In–Sb–Se alloy system. In our present work, we have studied the effect of Te content and thickness on optical parameters of $In_{35}Sb_{45}Se_{20-x}Te_x$ chalcogenide films with different compositions (x=2.5, 5, 7.5, 10, 12.5 and 15 at%).

2. Experimental procedures

The different compositions of $In_{35}Sb_{45}Se_{20-x}Te_x$ chalcogenide alloys were x=2.5, 5, 7.5, 10, 12.5 and 15 at%. prepared by the standard melt quenching method. Typical, 10 g total (per batch) of

* Corresponding author.
E-mail address: diab_a_k@yahoo.com (A.K. Diab).

0022-3697/$ - see front matter Published by Elsevier Ltd.
doi:10.1016/j.jpcs.2010.06.011

appropriate quantities of 99.999% pure indium (In), antimony (Sb), selenium (Se) and tellurium (Te) were weighed according to their atomic percentages and sealed in quartz ampoules in a vacuum of $\approx 10^{-5}$ Torr. The sealed ampoules were kept inside a furnace, where the temperature was increased up to 1000 K for about 24 h, at the end of which the ampoules were quenched in ice water to obtain the different compositions of $In_{35}Sb_{45}Se_{20-x}Te_x$. During the preparation the ampoules were continuously rotated to ensure complete mixing of the various constituents. Thin films of the considered ratios were prepared by an electron beam evaporation, in an Edward's high vacuum coating unit model 306 A at pressures 5×10^{-6} and 8×10^{-5} Torr before and during film deposition, respectively. The films were prepared on ultrasonically cleaned microscope glass slides held at room temperature.

The thickness (d) of the films ($\approx$25–150 nm) was controlled using digital film thickness monitor model TM 200 Maxtek. The deposition rate was $\approx$7 nm/s. The crystallographic structure of the as-prepared films was determined by X-ray diffraction using a Philips X'pert MRD diffractometer. CuKα radiation (λ=1.541837 Å) was used from the X-ray tube with grazing incidence. The angle of incidence was 0.75°. The optical transmittance (T) and reflectivity (R), used for calculating the optical constant, were obtained by a Jasco 570 double beam spectrophotometer in the wavelength (λ) range 200–2500 nm at normal incidence [21,22]. In order to exclude the effect of the substrate on transmission and reflection, a bare glass substrate was taken as a reference during the measurements.

Both, the homogeneity and compositional contents of the films have been checked using energy dispersive analysis of X-ray (EDAX) at different points. It was found that percentage ratios of the elements are around the values taken for the bulk form with an experimental error of $\pm$2%.

3. Results and discussion

3.1. XRD characterization

Fig. 1 shows XRD patterns of the investigated compositions in as-prepared thin film as a representative example of thickness 150 nm. It is found that the as-prepared compositions have amorphous or polycrystalline nature dependingt on Te content in the composition. The obtained pattern indicated that $In_{35}Sb_{45}Se_{17.5}Te_{2.5}$, $In_{35}Sb_{45}Se_{15}Te_5$ and $In_{35}Sb_{45}Se_{12.5}Te_{7.5}$ thin films are amorphous (Fig. 1; x=2.5, 5 and 7.5 at%, while in each

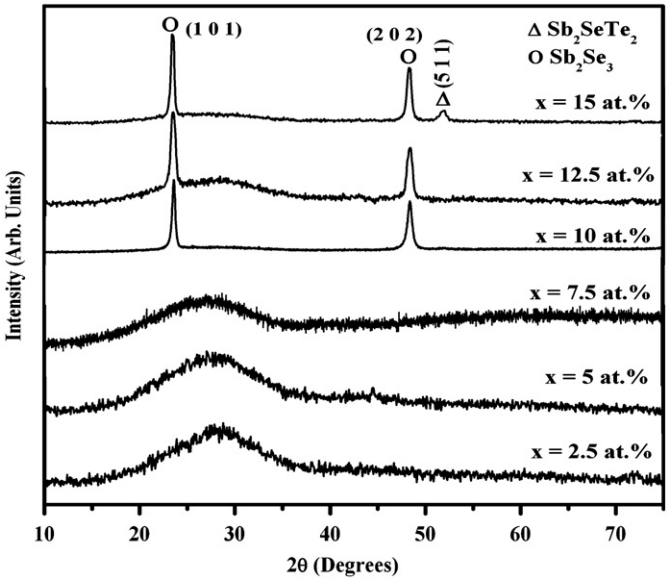

Fig. 1. X-ray diffraction patterns for the as-prepared $In_{35}Sb_{45}Se_{20-x}Te_x$ thin films of thickness d=150 nm.

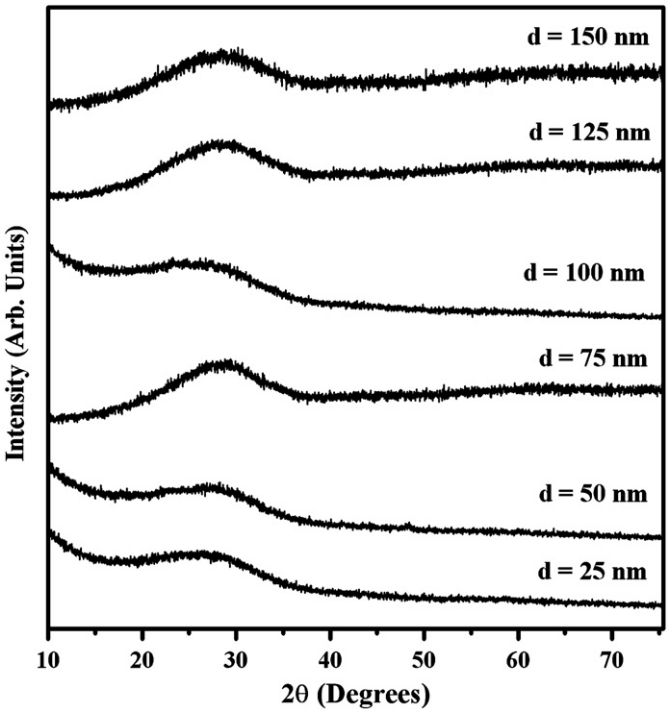

Fig. 2. X-ray diffraction patterns for the as-prepared $In_{35}Sb_{45}Se_{12.5}Te_{7.5}$ thin films of different thicknesses.

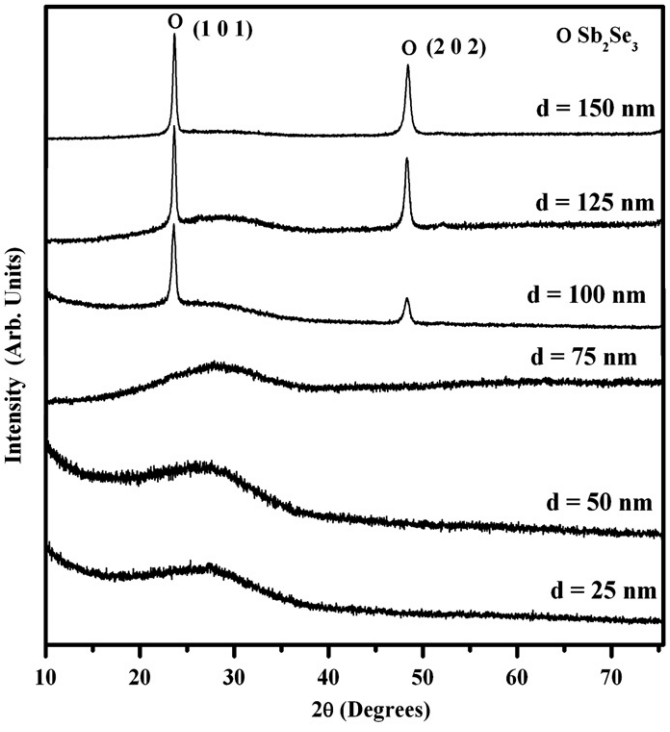

Fig. 3. X-ray diffraction patterns for the as-prepared $In_{35}Sb_{45}Se_{10}Te_{10}$ thin films of different thicknesses.

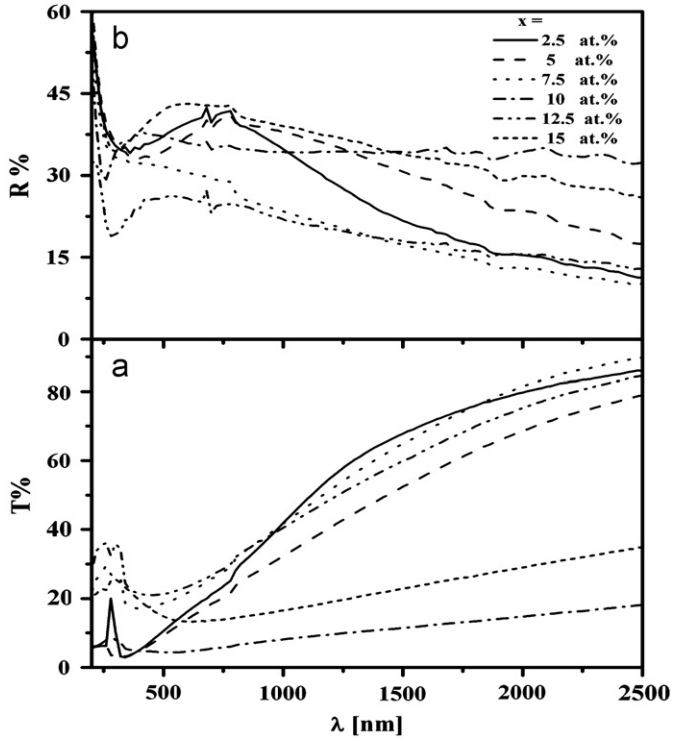

Fig. 4. Optical transmittance (a) and reflectance (b) spectra of 75 nm $In_{35}Sb_{45}Se_{20-x}Te_x$ films prepared with various Te contents.

$In_{45}Sb_{35}Se_{10}Te_{10}$, $In_{35}Sb_{45}Se_{7.5}Te_{12.5}$ and $In_{35}Sb_{45}Se_5Te_{15}$ patterns crystalline peaks are obtained (Fig. 1; $x=10$, 12.5 and 15 at%. From the JCPDS files, these peaks can be identified as Sb_2Se_3

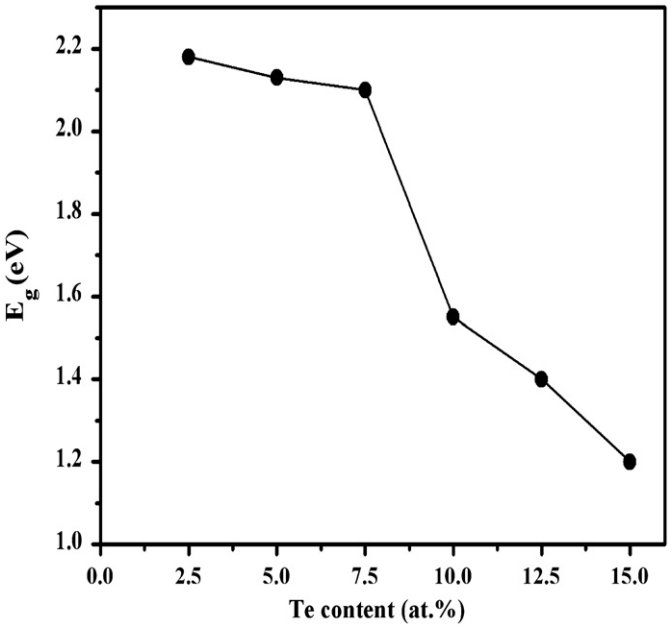

Fig. 6. Variation of optical band gap as a function of Te content. The solid line is a guide for the eye only.

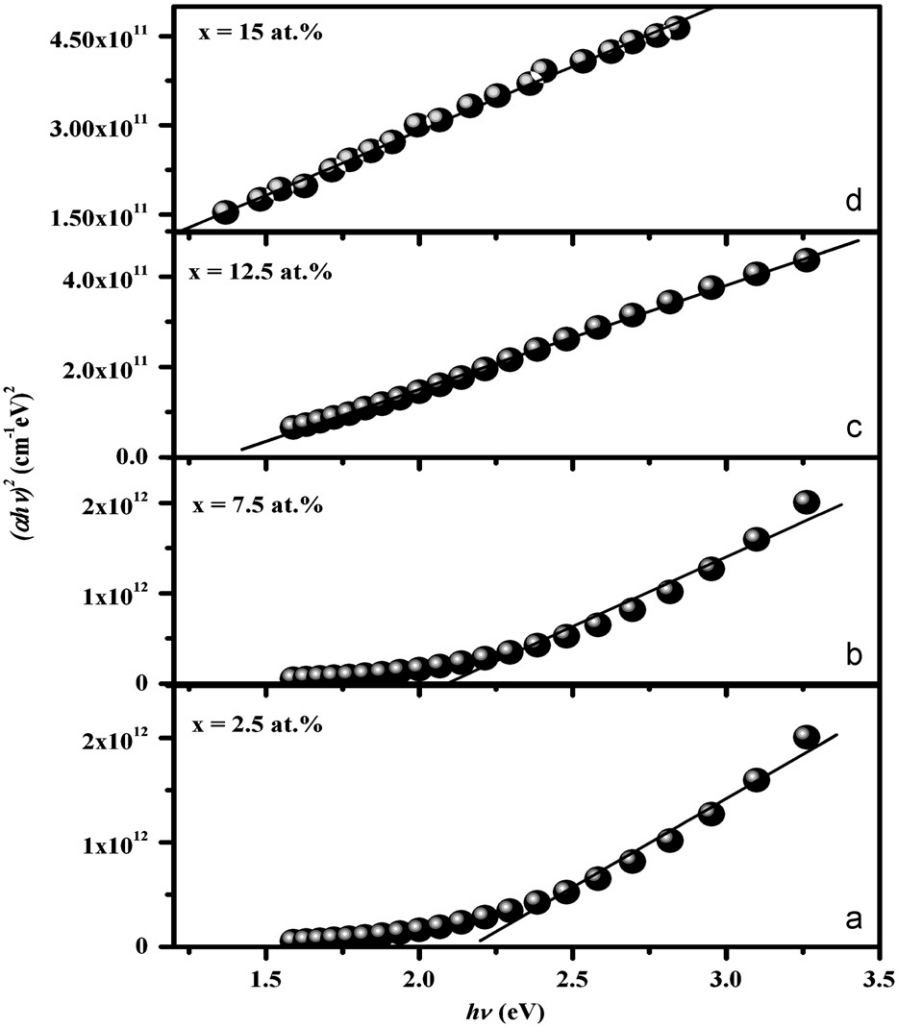

Fig. 5. $(\alpha h\nu)^2$ versus $h\nu$ for $In_{35}Sb_{45}Se_{20-x}Te_x$ thin films with thickness $d=150$ nm prepared of different Te contents.

(card nos. 22-0067 and 72-1184) and Sb_2SeTe_2 (card no.38-0979) crystalline phases.

The XRD patterns for $In_{35}Sb_{45}Se_{20-x}Te_x$ thin films with different thicknesses (d=25, 50, 75, 100, 125 and 150 nm) are shown in Figs. 2 and 3. It is found that the compositions with $x<10$ at% the films have an amorphous structure for all thicknesses see for example Fig. 2 for $In_{45}Sb_{35}Se_{12.5}Te_{7.5}$ with different thicknesses (d=25, 50, 75, 100, 125 and 150 nm). For $x\geq 10$ at% the films have an amorphous structure for thicknesses d=25, 50 and 75 nm (see for example (Fig. 3) (d=25, 50 and 75 nm) for $In_{35}Sb_{45}Se_{10}Te_{10}$, and crystalline peaks are obtained for films with thicknesses d=100, 125 and 150 nm Fig. 3 for the same composition). From the JCPDS files these peaks can be identified as Sb_2Se_3 (card nos. 15-0861 and 72-1184) crystalline phases and the intensity of these peaks increases with increase in film thickness.

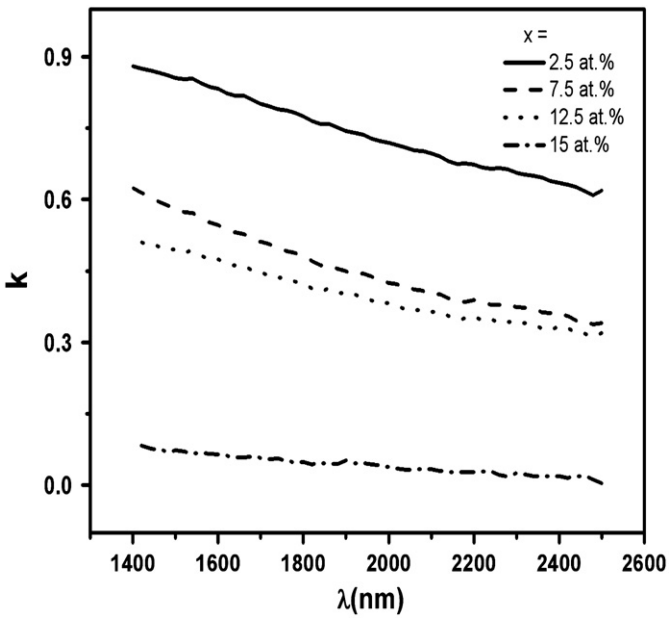

Fig. 7. Variation of extinction coefficient of the $In_{35}Sb_{45}Se_{20-x}Te_x$ (x=2.5, 7.5, 12.5and 15 at%) thin films prepared with thickness d=50 nm.

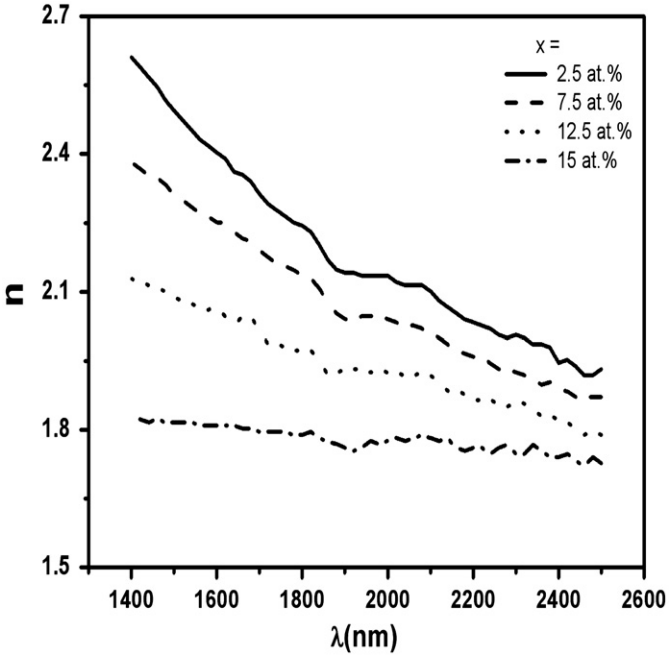

Fig. 8. Variation of refractive index of the $In_{35}Sb_{45}Se_{20-x}Te_x$ (x=2.5, 7.5, 12.5 and 15 at%) thin films prepared with thickness d=50 nm.

3.2. Optical properties of as-prepared films

3.2.1. Effect of composition

Fig. 4a and b shows the optical transmittance and reflectance spectra, respectively, of 75 nm $In_{35}Sb_{45}Se_{20-x}Te_x$ (where x=2.5, 5, 7.5, 10, 12.5 and 15 at%) films. As seen from Fig. 5a transmittance of the films is very high in the near infrared region (NIR) and decreases gradually with decrease in wavelength. The major feature in Fig. 4a and b appear to be a minimum in T and a maximum in R in the wavelength range 300–750 nm. These minima and maxima may be correlated to each other. It is further observed that there is a gradual decrease in transmittance around the optical band gap indicating that the films have defects.

Using the measured spectral transmittance and reflectance and film thickness (d) the absorption coefficient (α) was calculated according to the following relation [23]:

$$\alpha=\frac{1}{d}\ln\left[\frac{(1-R)^2}{T}\right] \quad (1)$$

The optical band gap (E_g) was determined using the following formula [24]:

$$\alpha h\upsilon=\beta(h\upsilon-E_g)^{\eta} \quad (2)$$

where β is a constant and η is equal to 2 or 1/2 for allowed indirect or direct transitions, respectively. The E_g values are extracted from the $(\alpha h\nu)^2$ versus $h\nu$ plot, indicating a direct band gap for all of examined $In_{35}Sb_{45}Se_{20-x}Te_x$ films.

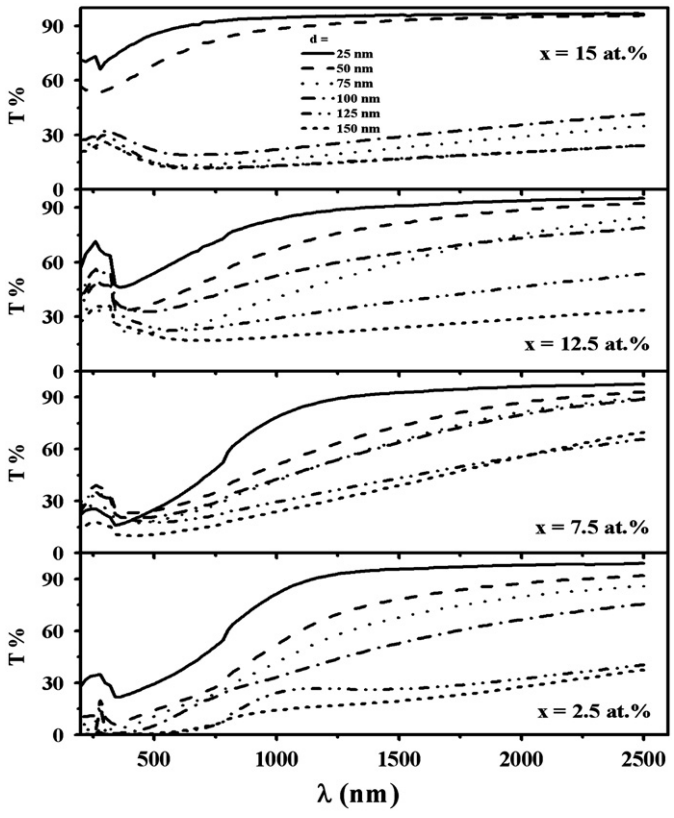

Fig. 9. Optical transmittance spectra of $In_{35}Sb_{45}Se_{20-x}Te_x$ films (x=2.5, 7.5, 12.5 and 15) prepared with various thicknesses (d=25, 50, 75, 100, 125 and 150 nm).

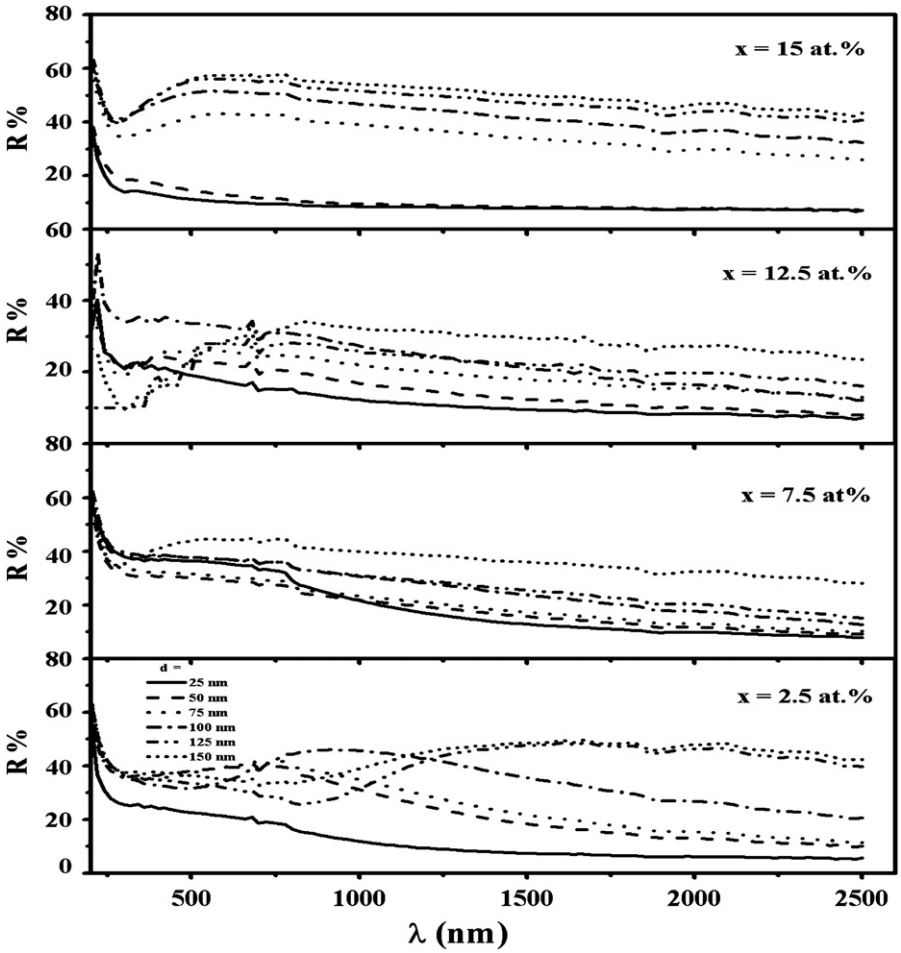

Fig. 10. Optical reflectance spectra of $In_{35}Sb_{45}Se_{20-x}Te_x$ films (x=2.5, 7.5, 12.5 and 15) prepared with various thicknesses (d=25, 50, 75, 100, 125 and 150 nm).

Fig. 5 shows the variation of $(\alpha h\nu)^2$ with $h\nu$ for thin films of thickness 150 nm obtained from optical absorption for the $In_{35}Sb_{45}Se_{20-x}Te_x$ prepared (where x=2.5, 7.5, 12.5 and 15 at%) films. The optical band gap values are calculated from the intercept of the linear part with the energy axis.

The optical band gap E_g has been determined by the intercept of the extrapolation to zero absorption with the photon energy axis ($\alpha h\nu^2 \rightarrow 0$, Tauc extrapolation) [25]. Fig. 6 shows that the optical band gap E_g is strongly dependent on the fractional concentration of Te atoms. The width of localized states near the mobility edge depends on the degree of disorder and defects present in the amorphous structure. Such defects are formed due to unsaturated bonds, which produce localized states in band gap. The presence of a high concentration of localized states in thin films is responsible for low optical band gap [26]. Therefore the addition of Te increases the concentration of localized states in the $In_{35}Sb_{45}Se_{20-x}Te_x$ compositions, leading to the decrease in band gap. The dominant contribution for the states near the valence band edge, in materials having chalcogen atoms as a major contribution, comes from chalcogen atoms, especially from their lone-pair p-orbital. The lone-pair electrons in these atoms adjacent to electropositive atoms will have higher energies than those close to the electronegative atoms. Therefore, the addition of electropositive elements to the alloy may raise the energy of some lone-pair states sufficiently to broaden further the band inside the forbidden gap. The electronegativities of In, Sb, Se and Te are 2, 1.9, 2.4 and 2.1, respectively. According to these values, it is noticed that Te is less electronegative than Se; consequently the substitution of Se by Te may raise the energy of some lone-pair states and hence broaden the valence band. This will give rise to additional absorption over a wider range of energy, leading to band tailing and hence shrinking the band gap. The same behavior has been reported by Othman et al. [27] for the $(As_{30}Sb_{15}Se_{55})_{100-x}Te_x$ films. The optical band gap of the $(As_{30}Sb_{15}Se_{55})_{100-x}Te_x$ films decreases while the width of localized states increases with increase in Te content.

The extinction coefficient k for all samples with different thicknesses has been calculated according to the following equation[28]:

$$k = \alpha\lambda/4\pi \tag{3}$$

The refractive index, n is related to optical reflectance R by the following relation [29,30]:

$$n = \frac{1+R}{1-R}\left[\left(\frac{R+1}{R-1}\right)^2 - (1+k^2)\right]^{1/2} \tag{4}$$

Figs. 7 and 8 show the variation of extinction coefficient and refractive index of $In_{35}Sb_{45}Se_{20-x}Te_x$ (x=2.5, 7.5, 12.5 and 15 at% as representative example) thin films, respectively, of thickness 50 nm. It is observed that the extinction coefficient and refractive index decrease with increase in Te content.

3.2.2. *Effect of thickness*

Figs. 9 and 10 show the spectral transmittance and reflectance, respectively, obtained at room temperature and at normal

incidence, for $In_{35}Sb_{45}Se_{20-x}Te_x$ films (x=2.5, 7.5, 12.5 and 15) with different thicknesses (d=25, 50, 75, 100, 125 and 150 nm), in the visible region. It is seen that transmittance decreases with increase in film thickness, while reflectance increase with increase in thickness for all the studied compositions. This may be related to the increase in defects, created from the difference in thermal expansion coefficients of the film and substrate, and to the increase in surface roughness with increase in film thickness.

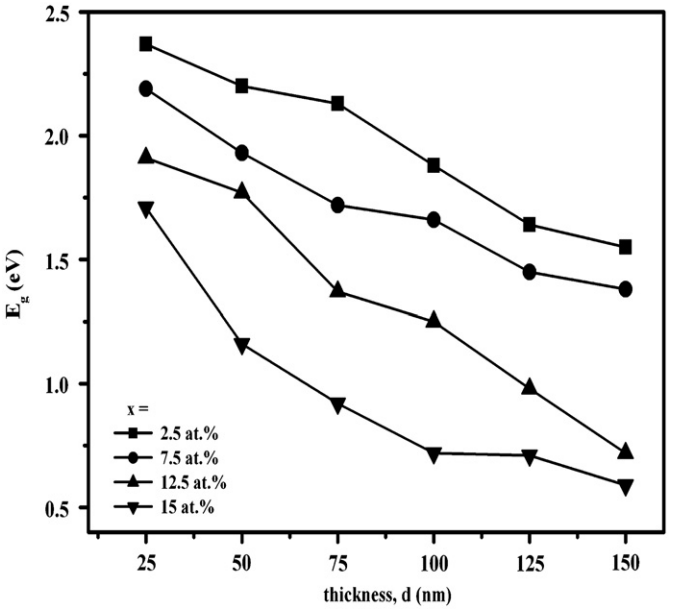

Fig. 11. Variations of optical band gap (E_g) with thickness d for as-prepared $In_{35}Sb_{45}Se_{20-x}Te_x$ thin films.

Fig. 11 shows the dependence of E_g on thickness of $In_{35}Sb_{45}Se_{20-x}Te_x$ thin films with x=2.5, 7.5, 12.5 and 15 at%. For each composition, E_g decreases with increase in film thickness. The thickness affects the optical band gap due to the change of some of the bonds, strain and dislocation density. This possibly changes the intercrossing interactions between localized In, Sb, Se and Te states and the extended band states [31]. Also, this can be attributed to the increase of the opaqueness of film with increase in film thickness.

Figs. 12 and 13 show the extinction coefficient and refractive index of $In_{35}Sb_{45}Se_{20-x}Te_x$ (x=2.5, 7.5, 12.5and 15 at%) thin films of different thicknesses (25, 50, 75, 100, 125 and 150 nm), respectively. The optical constants, n and k, were found to be dependent on film thickness in the investigated range. It is observed that the extinction coefficient and refractive index increase with increase in thickness for all the examined compositions.

The refractive index dispersion data in semiconductors have been analyzed using the concept of single oscillator. Using this concept the energy parameters E_d and E_o are introduced and the refractive index, n, at a photon energy E was expressed by Wemple and Di Domenicco [32] and Wemple [33] through the following relation:

$$(n^2-1)^{-1} = E_d E_o/(E_o^2-E^2) \quad (5)$$

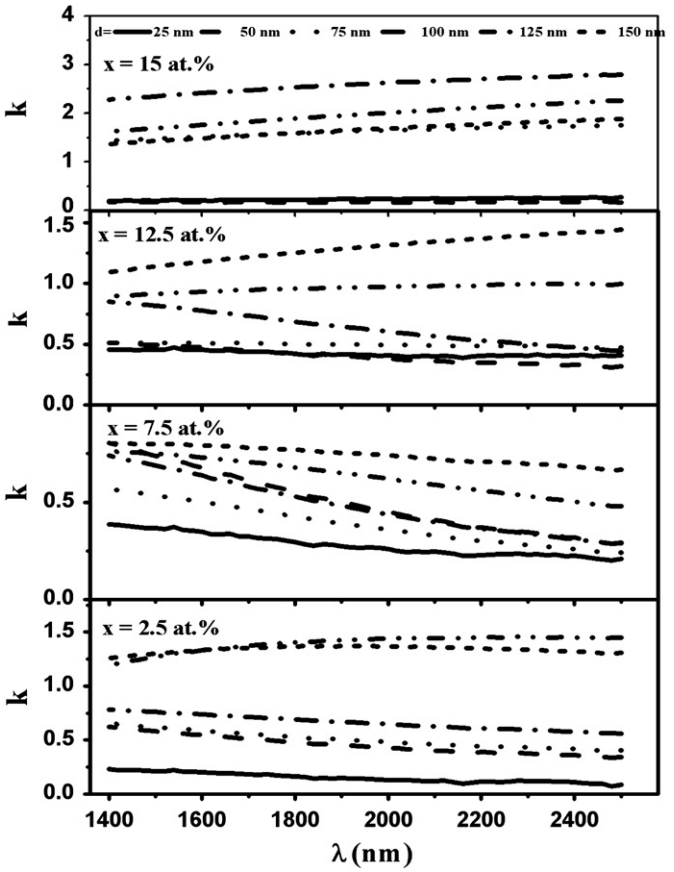

Fig. 12. Variation of extinction coefficient of the $In_{35}Sb_{45}Se_{20-x}Te_x$ (x=2.5, 7.5, 12.5and 15 at%) thin films prepared with different thicknesses (d=25, 50, 75, 100, 125 and 150 nm).

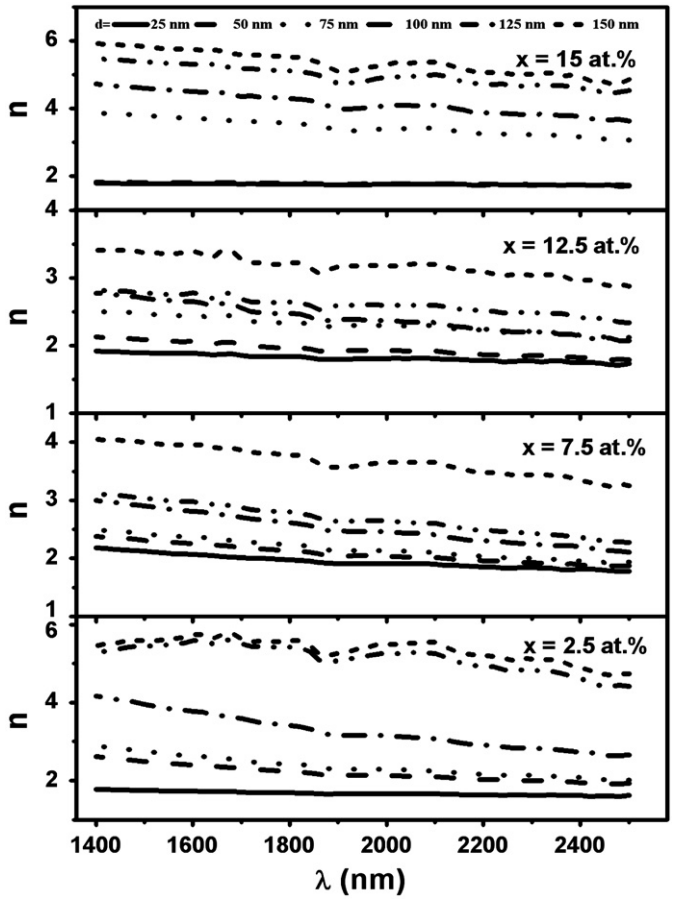

Fig. 13. Variation of refractive index of the $In_{35}Sb_{45}Se_{20-x}Te_x$ (x=2.5, 7.5, 12.5 and 15 at%) thin films prepared with different thicknesses (d=25, 50, 75, 100, 125 and 150 nm).

Table 1
Variations of N/m^*, ε_∞, E_d, E_o and ω_p of the as-deposited $In_{45}Sb_{35}Se_{20-x}Te_x$, thin films with different thicknesses (25, 50, 75, 100, 125 and 150 nm).

Thickness d (nm)	E_o (eV)	E_d (eV)	ε_∞	$(N/m^*)\times10^{-47}$ ($g^{-1}\,cm^{-3}$)	$\omega_p\times10^{-14}$ (s^{-1})
25	0.962	1.552	4.31838	2.32	5.11
50	0.895	1.538	4.89071	2.99	5.07
75	0.869	1.589	5.58489	3.85	4.83
100	0.8	1.75	8.02987	7.14	4.46
125	0.798	2.09	9.19395	8.31	4.20
150	0.87	5.708	17.28959	14.0	3.94

where E_d is the electronic dispersion energy and E_o the single oscillator energy. The physical meaning of the single-oscillator energy E_o is that it simulates all the electronic excitations involved and E_d is the dispersion energy, which is related to the average strength ofe optical transitions. In practice the dispersion parameters E_d and E_o can be obtained according to Eq. (5) by a simple plot of $(n^2-1)^{-1}$ versus E^2.

Using Drude's theory ofhe dielectrics, the real part ε' of the complex dielectric function ε can be written as [34]

$$\varepsilon' = n^2-k^2 = \varepsilon_\infty-[e^2N/\pi c^2m^*]\lambda^2 \quad (6)$$

where ε_∞ is the residual dielectric constant (high frequency component of the relative permittivity), c the light velocity, N and m^* are the free carrier concentration and its effective mass, respectively, and e is the electronic charge. Plasma resonance frequency for one kind of free carrier can be written as [35]

$$\omega_p = [e^2N/\varepsilon_0\varepsilon_\infty m^*]^{1/2} \quad (7)$$

where ε_o the free space dielectric constant.

Table 1 presents the variations of N/m^*, ε_∞, E_d, E_o and ω_p of the as-deposited $In_{35}Sb_{45}Se_{20-x}Te_x$, thin films with different thicknesses (25, 50, 75, 100, 125 and 150 nm). The table emphasized that, both N/m^*, ε_∞ and E_d increase with the increase of the film thickness, while E_o and ω_p decrease. This can be attributed to change in microstructure of films and extension of long range ordering in their structures.

4. Conclusions

XRD characteristics of films prepared by electron beam evaporation showed that the as-prepared composition has an amorphous or polycrystalline nature dependent on Te content in the composition and thickness. Optical transmittance and reflectance are found to be sensitive to film thickness. Optical transition in the films is found to be direct and permitted. E_g values decrease with increase in Te content and thickness. Different parameters like high frequency dielectric constant ε_∞, ratio N/m* and plasma frequency ω_p were determined by analysis of dispersion curve of refractive index.

Acknowledgments

The authors would like to acknowledge the scientific support of Dr. Sodky H. Mohamed and they thank him for his efforts.

References

[1] N. Yamada, E. Ohno, K. Nishiuchi, N. Akahira, M. Takao, J. Appl. Phys. 69 (1991) 2849.
[2] J.H. Coombs, A.P.J.M. Jongenelis, W. van Es-Spiekman, B.A.J. Jacobs, J. Appl. Phys. 78 (1995) 4906.
[3] C. Peng, L. Cheng, M. Mansuripur, J. Appl. Phys. 82 (1997) 4183.
[4] K. Nakayama, K. Kojima, F. Hayakawa, Y. Imai, A. Kitagawa, M. Suzuki, Jpn. J. Appl. Phys. Part I 39 (2000) 6157.
[5] S. Lai, T. Lowrey, in: Technical Digest of the International Electron Devices Meeting 01 (2001) 803.
[6] S.M. Yoon, N.Y. Lee, S.O. Ryu, K.J. Chio, Y.S. Park, S.Y. Lee, B.G. Yu, M.J. Kang, S.Y. Chio, M. Wuttig, IEEE Electron Device Lett. 27 (2006) 445.
[7] P. Arun, A.G. Vedeshwar, Mater. Res. Bull. 34 (1999) 203.
[8] H. Tashiro, M. Harigaya, Y. Kageyama, K. Ito, M. Shinotsuka, K. Tani, A. Watada, N. Yiwata, Y. Nakata, S. Emura, Jpn. J. Appl. Phys. 41 (2002) 3758.
[9] J. Li, F. Gan, Thin Solid Films 402 (2002) 232.
[10] S. Zwerding, B. Lax, Laura M. Roth, Phys. Rev. 108 (1957) 1402.
[11] E. Burstein, G.S. Picus, H.A. Gebbie, Phys. Rev. 103 (1956) 825.
[12] T.S. Moss, SD. Smith, T.D.F. Hawkins, Proc. Phys. Soc B70 (1957) 776.
[13] Yoshio Sato, Minemura Hiroyuki, Maeda Yoshihito, Ikuta Isao, Andoh Hisashi, Tsuboi Nobuyoshi, Nagai Masaichi, Proc. SPIE 1316 (1990) 267.
[14] Yoshito Meada, Isao Ikuta, Hisashi Andoh, Yoshio Sato, Jpn. J. Appl. Phys. 31 (1992) 451.
[15] G. Kaur, T. Komatsu, J. Mater. Sci. 36 (2001) 4531.
[16] M.S. Kanboj, G. Kaur, R Thangaraj, D.K. Avasthi, J. Appl. Phys. 35 (2002) 477.
[17] D. Eddike, A. Ramdani, G. Brun, J.C. Tedenac, B. Liautard, Mater. Res. Bull. 33 (1998) 519.
[18] N.M. Gasanly, B.A. Natiy, A.E. Bakhyshor, K.G. Shirinov, Phys. Status Solidi 153 (1989) k89.
[19] T. Ohta, J. Optoelectron. Adv. Mater. 3 (2001) 609.
[20] V.M. Rubish, P.P. Shtets, V.V. Rubish, D.G. Semak, B.R. Tsizh, J. Optoelectron. Adv. Mater. 5 (2003) 1193.
[21] S.H. Mohamed, M.M. Wakkad, A.M. Ahmed, A.K. Diab, Eur. Phys. J. Appl. Phys. 34 (2006) 165–171.
[22] M.M. Wakkad, E.Kh. Shokr, H.A. Abd El Gani, M.A. Awad, Eur. Phys. J. Appl. Phys. 43 (2008) 23–30.
[23] T.S. Moss, in: Optical Properties of Semiconductors, Academic press, New York, 1959 p. 40.
[24] R.A. Smith, in: Semiconductors, Second ed., Cambridge University Press, London, 1978.
[25] J. Tauc, A. Menth, J. Non-Cryst. Solids 8 (1972) 569.
[26] Pankaj Sharma, S.C Katyal, Mater. Lett. 61 (2007) 4516.
[27] A.A. Othman, K.A. Aly, A.M. Abousehly, Thin Solid Films 515 (2007) 3507.
[28] E. Marquez, J. Ramirez, P. Villares, R. Jimenez, P.J.S. Ewen, A.E. Owen, J. Phys. D 25 (1992) 535.
[29] M. Becker, H.Y. Fan, Phys. Rev. 76 (1949) 1530.
[30] T.S. Moss, in: Optical Properties of Semiconductors, Academic Press, New York, 1959.
[31] J. Wu, W. Walukiewicz, K.M. Yu, J.W. Ager III, E.E. Haller, I. Miotkowski, A.K. Ramdas, C.-H. Su, I.K. Sou, R.C.C. Perera, J.D. Denlinger, Phys. Rev. B 67 (2003) 035207.
[32] S.H. Wemple, M. Didomenico, Phys. Rev. B 3 (1971) 1338.
[33] S.H. Wemple, Phys. Rev. B 7 (1973) 3767.
[34] M.M. El-Nahass, A.A. Farag, E.M. Ibrahim, S. Abd El-Rahman, Vacuum 72 (2004) 453.
[35] J. Robert, A. Mark, W. Alexander, J. Appl. Opt. 24 (1985) 22.